

## The selectivity of electrosynthesised polymer membranes depends on the electrode dimensions: implications for biosensor applications

Colm P. McMahon, Sarah J. Killoran, Sarah M. Kirwan and Robert D. O'Neill\*

Chemistry Department, University College Dublin, Belfield, Dublin 4, Ireland.

E-mail: Robert.O'Neill@UCD.ie; Fax: +353-1-7162127; Tel: +353-1-7162314

Received (in Cambridge, UK) 27th May 2004, Accepted 24th June 2004

First published as an Advance Article on the web 2nd August 2004

A biosensor selectivity coefficient defined for poly(*o*-phenylenediamine) electrosynthesised onto Pt microdisks and cylinders was unexpectedly found to change as the scale of the electrodes decreased, mainly due to enhanced permeability of a ubiquitous interference species in biological systems, ascorbic acid.

Electrode modifications incorporating biological elements, such as cells and enzymes, to produce biosensors has become an important strategy in electroanalytical chemistry. The classic<sup>1</sup> and most common<sup>2</sup> enzyme-modified electrode is the glucose biosensor incorporating the oxidoreductase enzyme, glucose oxidase (GOx). This type of sensor has become the model system primarily due to the importance of glucose monitoring in the disease diabetes mellitus, and the fact that glucose determination in various body fluids, such as blood, plasma and urine, remains one of the most common analyses performed in clinical laboratories. Although the presence of the enzyme provides sensitivity to the target analyte, biosensors must also have excellent interference rejection characteristics to be useful in real applications. This selectivity is usually achieved by the inclusion of a permselective membrane in the biosensor design, which also serves to immobilise the enzyme and to protect the electrode surface from fouling. The types of membrane used include pre-cast (e.g., cellulose acetate) and cast (e.g., Nafion) coatings, and more recently, entrapment within electrosynthesised polymeric matrices (e.g., polypyrrole and polyphenylenediamines).<sup>3–6</sup> The quantitative significance of the selectivity depends on the relative concentrations of the target analyte and interference. For example, despite the high concentration of the main interference species, ascorbic acid (AA, 500  $\mu\text{M}$ ), reliable monitoring of glucose ( $\sim 400 \mu\text{M}$ ) in brain extracellular fluid (ECF) has been achieved, using GOx-modified Pt and poly(*o*-phenylenediamine), PPD, as the interference barrier.<sup>2</sup> In contrast, the present Pt/PPD-enzyme biosensor design does not appear to be suitable for detecting ECF glutamate because the corresponding concentrations of this neurotransmitter are about two orders of magnitude lower than that of AA.<sup>7</sup> Thus, further developments in biosensor design are essential to broaden the range of analytes accessible to real-time, long-term monitoring *in vivo*. One of the key design features of *in-vivo* probes is their dimension, which needs to be minimised in order to minimise tissue damage. However, a common strategy is to characterise sensor designs using macro-electrodes, with the aim of scaling down at a later stage. Here we report an unexpected outcome of changing the size of the electrode substrate on properties of electrosynthesised polymer coatings.

We define the selectivity coefficient,  $S\%$ , in terms of the current recorded for 1 mM of each of: the oxidase signal transduction molecule,  $\text{H}_2\text{O}_2$ ,  $\text{I}(\text{H}_2\text{O}_2)$ ; and the interference species with the highest concentration in most biological tissues and fluids, especially brain ECF, AA,  $\text{I}(\text{AA})$ . The  $S\%$  value was calculated as the percentage interference,  $100 \cdot \text{I}(\text{AA})/\text{I}(\text{H}_2\text{O}_2)$ , because  $\text{I}(\text{AA})$  is very small compared with  $\text{I}(\text{H}_2\text{O}_2)$  and is ideally zero; thus the optimum value of  $S\%$  defined in this way is zero.<sup>8</sup> The use of equimolar concentrations in this definition allows  $S\%$  to be interpreted in terms of the ratio of effective polymer permeability for two analytes with the same  $z$ -value (electrons transferred per molecule), as is the case for AA and  $\text{H}_2\text{O}_2$  ( $z = 2$ ). Recently, we

reported a benchmark value of  $S\% = 0.15\%$  for Pt cylinders ( $\text{Pt}_\text{C}$ , 60- $\mu\text{m}$  radius, 1-mm length) modified with a PPD-globular protein (GP, bovine serum albumin) composite electrosynthesised amperometrically, indicating excellent selectivity of  $\text{Pt}_\text{C}/\text{PPD-GP}$  electrodes. This resulted from a combination of high sensitivity (current) for  $\text{H}_2\text{O}_2$  (similar to bare Pt) and low permeability of AA through the PPD-GP matrix. Indeed, of a broad range of electrogenerated AA-blocking polymers investigated in a number of studies, PPD is distinguished by its high permeability to  $\text{H}_2\text{O}_2$ .<sup>8–10</sup> GP was incorporated into the polymer during electrosynthesis to model the enzyme present in biosensors and to improve the polymer's AA-rejecting characteristics;<sup>8,11</sup> different GPs tested (GOx, bovine serum albumin, egg albumin, etc.) were indistinguishable in this respect.<sup>12</sup>

Although 1-mm long cylinder wire biosensors are adequate for *in-vivo* neurochemical studies of relatively large brain regions, such as the dorsal striatum,<sup>13</sup> smaller electrodes are required for small regions and for studying layers of cells within regions, such as the cerebral cortex. Thus,  $\text{Pt}_\text{D}/\text{PPD-GP}$  disk electrodes were fabricated by cutting the Teflon<sup>®</sup>-coated Pt wire transversely to produce 60- $\mu\text{m}$  radius Pt disks ( $\text{Pt}_\text{D}$ ), and electropolymerisation carried out at 700 mV vs. SCE in 300 mM 1,2-diaminobenzene in quiescent phosphate buffered saline (PBS, pH 7.4) containing 5 mg mL<sup>-1</sup> bovine serum albumin, as described previously for cylinders.<sup>8</sup> After rinsing and a settling period at 700 mV in fresh PBS, calibrations were carried out to determine the sensitivity of the  $\text{Pt}_\text{D}/\text{PPD-GP}$  disk electrodes to AA.

The calibrations for AA at  $\text{Pt}_\text{D}/\text{PPD-GP}$  electrodes were of the typical non-linear form reported and discussed for standard  $\text{Pt}_\text{C}/\text{PPD-GP}$  cylinder electrodes;<sup>8,11</sup> see Fig. 1. Remarkably, however, the current density for AA was an order of magnitude greater at  $\text{Pt}_\text{D}/\text{PPD-GP}$  compared with  $\text{Pt}_\text{C}/\text{PPD-GP}$  electrodes. This behaviour was not due to the classical difference between hemispherical and cylindrical diffusion at the two electrode geometries because AA sensitivity at the bare  $\text{Pt}_\text{D}$  metal was less than a factor of two greater than that for bare  $\text{Pt}_\text{C}$  in CV experiments ( $80 \pm 10\%$  at the reversal potential, 800 mV). Four characteristic features of calibration plots, such as those shown in Fig. 1, have been

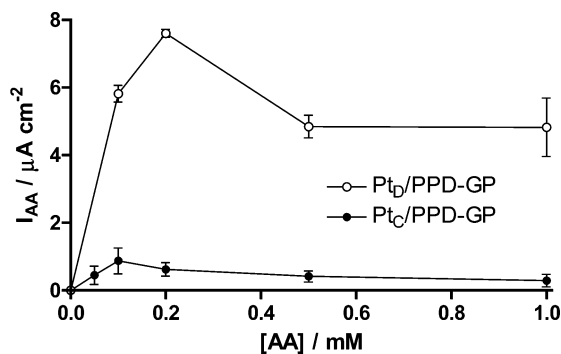


Fig. 1 Ascorbate calibration plots, expressed as current densities, recorded at Pt/PPD-GP electrodes of different geometries ( $\text{Pt}_\text{D}$  and  $\text{Pt}_\text{C}$ ).  $\text{Pt}_\text{C}$  = 1 mm cylinders of 125  $\mu\text{m}$  diameter ( $n = 23$ );  $\text{Pt}_\text{D}$  = 125- $\mu\text{m}$  diameter disks ( $n = 6$ ). Mean  $\pm$  s,  $n$  = number of electrodes.

identified,<sup>8</sup> here, however, the plateau current at 1 mM AA is sufficient to compare quantitatively AA blocking of the different polymer-modified electrodes. All AA sensitivities below are given as this 1 mM value.

Although the blocking ability of Pt<sub>D</sub>/PPD-GP disk electrodes was considerably poorer than that of the corresponding cylinder geometry, the PPD-GP composite formed on the disk well enough to reduce the AA sensitivity by two orders of magnitude compared with the bare disk. Expressed as a current density, the sensitivity of the Pt<sub>D</sub>/PPD-GP disk electrodes ( $1.5 \pm 0.3 \mu\text{A cm}^{-2}$ ,  $n = 6$ ) was significantly less than for bare (unmodified) Pt<sub>D</sub> electrodes ( $135 \pm 10 \mu\text{A cm}^{-2}$ ,  $n = 6$ ) for 1 mM AA, but greater than that for the corresponding cylinder geometry ( $0.20 \pm 0.02 \mu\text{A cm}^{-2}$ ,  $n = 6$ );  $P < 0.002$ . It appears, therefore, that the PPD layer did form on the disk, but that its ability to block AA was compromised relative to Pt<sub>C</sub>/PPD-GP electrodes.

Given this unexpected result, a range of electrode sizes and geometries (disks and cylinders) were tested. The PPD-GP polymer-protein composite was deposited as described above onto: 1.6-mm diameter disks; 0.2 mm cylinders of 125  $\mu\text{m}$  diameter; and 125- $\mu\text{m}$  diameter disks. The 1 mM AA sensitivity was then determined and compared with present and literature values<sup>8</sup> for 1 mm cylinders of 125  $\mu\text{m}$  diameter; see Fig. 2.

The data in Fig. 2 show that the PPD-GP coating formed on all sizes of Pt electrodes investigated. Even the poorest AA blocking case (125- $\mu\text{m}$  diameter disks) gave 1 mM AA current densities ( $j$ ,  $1.5 \pm 0.3 \mu\text{A cm}^{-2}$ ,  $n = 6$ ) that were greatly below the value for the bare electrode ( $135 \pm 10 \mu\text{A cm}^{-2}$ ,  $n = 6$ ). Fig. 2 also shows that the AA-rejecting ability of the PPD-GP layer was significantly greater when it was formed on larger electrodes, such as the 1 mm cylinder ( $P < 0.002$ ). Area rather than geometry appears to be the determining factor here because the plot of  $I(\text{AA})$  vs. area was monotonic, and because the first and last points were both disks (Fig. 2). These data support the suggestion above that the AA-blocking characteristics of PPD-GP coatings formed on Pt surfaces of different dimensions are compromised as the electrode size diminishes. Since it is possible that H<sub>2</sub>O<sub>2</sub> sensitivity also changes under these conditions, H<sub>2</sub>O<sub>2</sub> calibrations were carried out on a variety of Pt/PPD-GP geometries, and values of S% (defined above) calculated. The results are shown in Fig. 3.

There was no systematic trend in the H<sub>2</sub>O<sub>2</sub> sensitivity for the difference geometries, and the variation in the S%-value shown in Fig. 3 mainly reflects differences in AA responses shown in Fig. 2. Overall, there was a factor of ten between the S% value for the 1 mm cylinder compared with the corresponding disk electrode, the smaller electrodes being less selective. There was no significant difference between the S% calculated for the two populations of 1-mm long cylinder electrodes used in these discussions (literature,<sup>8</sup>  $n = 23$ , and present,  $n = 6$ ,  $P > 0.92$ ).

To investigate the cause of the altered properties of PPD-GP deposited on Pt of different dimensions, we analysed the current flowing during the electropolymerisation process for the two extreme cases (Fig. 2): 1.6-mm diameter macro-disks (Pt<sub>M</sub>) and

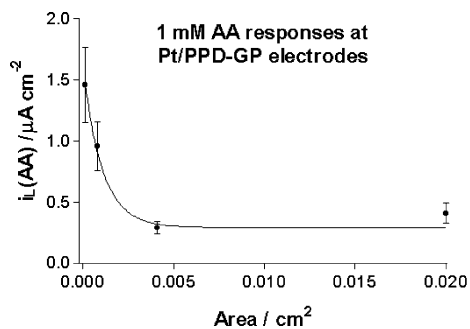


**Fig. 2** Current densities for 1 mM AA (see Fig. 1) recorded at Pt/PPD-GP electrodes of different sizes plotted against total electrode area. From the right: 1.6-mm diameter disks ( $n = 5$ ); 1 mm cylinders of 125  $\mu\text{m}$  diameter ( $n = 23$ ); 0.2 mm cylinders of 125  $\mu\text{m}$  diameter ( $n = 4$ ); and 125- $\mu\text{m}$  diameter disks ( $n = 6$ ). Mean  $\pm$  SEM,  $n =$  number of electrodes.

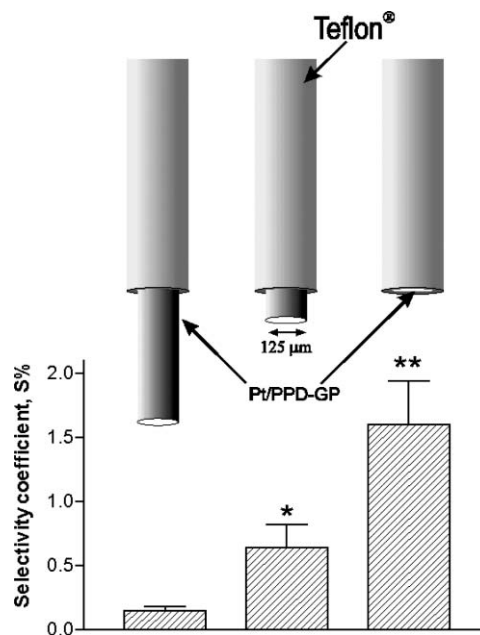


**Fig. 3** Selectivity coefficient,  $S\% = 100 \cdot I(\text{AA})/I(\text{H}_2\text{O}_2)$ , determined for three different Pt/PPD-GP dimensions. From the left: 1 mm cylinders of 125  $\mu\text{m}$  diameter ( $n = 23$ ); 0.2 mm cylinders of 125  $\mu\text{m}$  diameter ( $n = 4$ ); and 125- $\mu\text{m}$  diameter disks ( $n = 6$ ). Mean  $\pm$  SEM,  $n =$  number of electrodes. The differences were statistically significant with  $P < 0.001$  (\*) and  $P < 0.05$  (\*\*) when compared with the data to the immediate left.

125- $\mu\text{m}$  diameter disks, Pt<sub>D</sub>. The mechanism of formation and the structure of electrochemically generated PPD are complex and have been studied in some detail.<sup>11,14-17</sup> The properties of PPD depend strongly on the conditions of the polymerisation, such as pH, electrolyte composition and the voltage profile used. PPD generated at neutral pH forms a non-conducting, self-sealing coating on Pt<sup>8,11,18,19</sup> and other electrode materials.<sup>19-23</sup> Thus, the electropolymerisation current recorded amperometrically at +700 mV decays as the polymer grows and blocks further monomer oxidation, as shown in Fig. 4. The data for both Pt<sub>M</sub> and Pt<sub>D</sub> electrodes fitted one-phase exponential decay well, with  $R^2 > 0.98$  (Fig. 4). However, there were significant differences between the time-course of the decays: the half-life for Pt<sub>D</sub> ( $1.0 \pm 0.1$  s,  $n = 4$ ) was smaller than that for Pt<sub>M</sub> ( $10 \pm 2$  s,  $n = 4$ ); in addition, the current density passed during the first few seconds was higher for Pt<sub>D</sub> (see Fig. 4). We propose that the more efficient (hemispherical) diffusion of monomer to the Pt<sub>D</sub> surface gives rise to the initial high current density and fast polymer formation

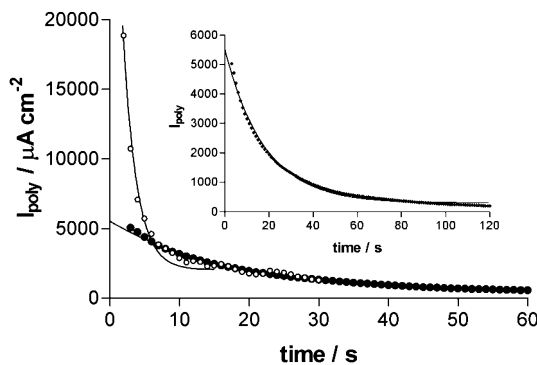


**Fig. 4** The first 1 min of the PPD electropolymerisation currents, expressed as current densities, recorded in PBS with 300 mM monomer at 700 mV vs. SCE, using a large stainless steel rod as auxiliary and two types of working electrode: 1.6-mm diameter macro-disks (Pt<sub>M</sub>, filled circles) and 125- $\mu\text{m}$  diameter disks (Pt<sub>D</sub>, open circles). The curves represent one-phase exponential decays calculated using non-linear regression, all  $R^2 > 0.98$ . Total recording time was 15 min. **Inset:** Enhanced detail of the data for the Pt<sub>M</sub> electrode.

that self-blocks rapidly. The less efficient linear diffusion at the Pt<sub>M</sub> electrode leads to smaller initial current densities and slower self sealing. We speculate that the very fast polymer deposition observed at Pt<sub>D</sub> electrodes is too rapid to allow the compact ordering of the PPD strands suggested for polymers synthesised onto surfaces,<sup>24</sup> leading to greater AA permeability in subsequent calibration experiments (see Figs. 1 and 2). The slower polymer deposition observed at Pt<sub>M</sub> electrodes (Fig. 4) and at Pt<sub>C</sub> cylinders (data not shown), allows for more orderly and compact PPD formation.

Finally, to determine whether this electrode size-dependent polymer growth phenomenon applied to other electrosynthesised polymers, polyphenol (PP) was synthesised in a similar way to PPD to form Pt<sub>C</sub>/PP and Pt<sub>D</sub>/PP modified electrodes. It has been shown that PP forms even thinner coatings (~3 nm) than PPD under these conditions,<sup>9,25</sup> and that GPs undermine its AA-rejecting properties;<sup>9</sup> therefore no GP was added to the phenol monomer solution. AA calibrations similar to those presented in Fig. 1 were carried out for Pt<sub>C</sub>/PP and Pt<sub>D</sub>/PP electrodes. The difference between the two electrode sizes was even more marked for PP-modified Pt, with two orders of magnitude separating their ability to block AA. These results also show that the additional complication of GPs present in the case of PPD does not play a vital role in the differences observed between Pt<sub>C</sub>/PPD-GP and Pt<sub>D</sub>/PPD-GP electrodes.

These results have important implications for the development of biosensors for biological applications where miniaturisation is a key goal. Apparently, it is not sufficient to model a design on large electrodes and then scale down, hoping to maintain selectivity characteristics, with the assumption that the sensitivity to different species scales in the same proportion. Here we show that polymer formation is adversely affected by reducing the electrode size, leading to significantly poorer selectivity (Fig. 3).

The mechanism of altered polymer formation is unclear. The very fast self-sealing reaction associated with PPD formation<sup>18,22,26</sup> could be sensitive to differences in transport profiles in the monomer solution, especially since both diffusion towards and away from the electrode may be involved in polymer growth.<sup>27</sup> We are presently investigating these factors and exploring a variety of polymerisation conditions to improve the selectivity of polymer films formed on microelectrodes. Atomic force microscopy will play an important role in exploring the differences between polymer structures formed on electrodes of different sizes. Irrespective of the mechanisms involved, however, it is the phenomenological properties of these polymers that are of prime importance in their applications, such as for permselective membranes in biosensor design.

We thank Enterprise Ireland for a postgraduate research award (CMcM) and UCD for financial support.

## Notes and references

- 1 L. C. Clark, Jr. and C. Lyons, *Ann. N. Y. Acad. Sci.*, 1962, **102**, 29–45.
- 2 R. D. O'Neill and J. P. Lowry, in *Encyclopedia of Analytical Chemistry*, ed. R. Meyers, John Wiley & Sons Ltd., Chichester, 2000, pp. 676–709.
- 3 A. P. F. Turner, I. Karube and G. S. Wilson, *Biosensors: Fundamentals and Applications*, Oxford University Press, New York, 1987.
- 4 A. E. G. Cass, *Biosensors: A Practical Approach*, Oxford University Press, New York, 1990.
- 5 P. Pantano and W. G. Kuhr, *Electroanalysis*, 1995, **7**, 405–416.
- 6 R. D. O'Neill, J. P. Lowry and M. Mas, *Crit. Rev. Neurobiol.*, 1998, **12**, 69–127.
- 7 J. P. Lowry, M. R. Ryan and R. D. O'Neill, in *Monitoring Molecules in Neuroscience*, eds. W. T. O'Connor, J. P. Lowry, J. J. O'Connor and R. D. O'Neill, National University of Ireland, Dublin, 2001, pp. 70–71.
- 8 J. D. Craig and R. D. O'Neill, *Analyst*, 2003, **128**, 905–911.
- 9 J. D. Craig and R. D. O'Neill, *Anal. Chim. Acta*, 2003, **495**, 33–43.
- 10 L. J. Murphy, *Anal. Chem.*, 1998, **70**, 2928–2935.
- 11 J. P. Lowry and R. D. O'Neill, *Electroanalysis*, 1994, **6**, 369–379.
- 12 S. M. Kirwan and R. D. O'Neill, in *Monitoring Molecules in Neuroscience*, eds. J. Kehr, K. Fuxe, U. Ungerstedt and T. Svensson, Karolinska University Press, Stockholm, 2003, pp. 440–442.
- 13 M. Fillenz, J. P. Lowry, M. G. Boutelle and A. E. Fray, *Acta Physiol. Scand.*, 1999, **167**, 275–284.
- 14 I. Losito, F. Palmisano and P. G. Zambonin, *Anal. Chem.*, 2003, **75**, 4988–4995.
- 15 L. L. Wu, J. Luo and Z. H. Lin, *J. Electroanal. Chem.*, 1997, **440**, 173–182.
- 16 B. X. Ye, W. M. Zhang and X. Y. Zhou, *Chin. J. Chem.*, 1997, **15**, 343–352.
- 17 Y. Ohnuki, H. Matsuda, T. Ohsaka and N. Oyama, *J. Electroanal. Chem.*, 1983, **158**, 55–67.
- 18 J. M. Cooper, P. L. Foreman, A. Glidle, T. W. Ling and D. J. Pritchard, *J. Electroanal. Chem.*, 1995, **388**, 143–149.
- 19 D. Centonze, C. Malitesta, F. Palmisano and P. G. Zambonin, *Electroanalysis*, 1994, **6**, 423–429.
- 20 E. De Giglio, I. Losito, L. Torsi, L. Sabbatini and P. G. Zambonin, *Ann. Chim.*, 2003, **93**, 209–221.
- 21 E. Ekinci, G. Erdogdu and A. E. Karagozler, *J. Appl. Polym. Sci.*, 2001, **79**, 327–332.
- 22 P. N. Bartlett, P. R. Birkin, J. H. Wang, F. Palmisano and G. De Benedetto, *Anal. Chem.*, 1998, **70**, 3685–3694.
- 23 R. D. O'Neill, S. C. Chang, J. P. Lowry and C. J. McNeil, *Biosens. Bioelectron.*, 2004, **19**, 1521–1528.
- 24 I. Sapurina, A. Y. Osadchev, B. Z. Volchek, M. Trchova, A. Riede and J. Stejskal, *Synth. Met.*, 2002, **129**, 29–37.
- 25 D. W. M. Arrigan and P. N. Bartlett, *Biosens. Bioelectron.*, 1998, **13**, 293–304.
- 26 J. Wang, L. Chen, J. Liu and F. Lu, *Electroanalysis*, 1996, **8**, 1127–1130.
- 27 M. C. Demartinez, O. P. Marquez, J. Marquez, F. Hahn, B. Beden, P. Crouigneau, A. Rakotondrainibe and C. Lamy, *Synth. Met.*, 1997, **88**, 187–196.